Electronic Supplementary Material (ESI) for Journal of Materials Chemistry A.

Supporting Information

Revealing the Role of Defects in Graphene Oxide on Evolution of Magnesium Nanocrystals and the Resulting Effects on Hydrogen Storage

Dong Ju Han[†], Sangtae Kim[‡], Eun Seon Cho[*†]*

† Department of Chemical and Biomolecular Engineering, Korea Advanced Institute of Science and Technology (KAIST), Daejeon 34141, Republic of Korea

‡ Department of Nuclear Engineering, Hanyang University, Seoul 04763, Republic of Korea

SUPPLEMENTARY DISCUSSION

Control of defect density levels on the GO

The Fourier transform infrared spectroscopy (FT-IR) showed diminished oxygen-related peaks including O-H (~3200-3400 cm^{-1}), C=O (1725 cm^{-1}), C-OH (1380 cm^{-1}), C-O-C (1185 cm^{-1}), and C-O (1045 cm^{-1}), as the pristine GO was more reduced (**Figure S2a**). From the X-ray diffraction (XRD) spectra, it is revealed that the interlayer distance of reduced GO becomes narrower than that of the pristine GO (from 8.1 Å to 3.2 Å) (**Figure S3**). With regard to the morphology of the rGO, the lateral size was consistently maintained, although more reduced GO has a wrinkled structure compared to the initial state (**Figure S4**).

Ab initio computations

We first obtained the equilibrium lattice parameters and atomic positions of single-layer graphene. Upon making a supercell with 50 carbon atoms, defects were introduced to the graphene at the fixed (pristine graphene's) lattice parameters (**Figure S17**). The defect types included ketone-type oxygen adsorbates and hydroxides adsorbed on a carbon vacancy. The defect concentrations of 1 defect per 50 carbon atoms and 2 defects per 50 carbon atoms were specifically compared. For the latter defect concentration, three distinct defect configurations were pre-relaxed in terms of ionic positions, and the lowest-energy configuration was selected for the subsequent Mg adsorption. In order to account for more realistic defect densities, we also prepared modelled graphene oxides with the ratio of oxidized carbon to non-oxidized carbon at 3:7 and 5:5.

On the graphene derivatives, each Mg was added and relaxed in terms of ionic positions at the fixed graphene lattice parameters. To determine where Mg adsorbs on the defected and pristine graphene, we compute 50 distinct configurations for the first Mg added, and selected the lowest energy configuration. On the fully relaxed Mg-adsorbed graphene derivatives, each additional Mg was added by computing 39 distinct configurations and selecting the lowest energy configurations. Up to 15 Mg atoms were added to the prepared graphene derivatives. The average adsorption energy and the free energy of the Mg particle for all the configurations were plotted in **Figure S18**.

Classical nucleation theory formalism

The chemical potential of magnesium adsorbed on graphene is computed using *ab initio* calculations as the following:

$$\mu(Mg\ @\ C) = \frac{[E(n\ Mg\ on\ defected\ graphene) - E(defected\ graphene)]}{n} - TS(x)$$

where n stands for the number of Mg adsorbed, T the temperature and $S(x)$ the configurational entropy. Since the experimental synthesis occurred at room temperature, T was set to 298 K. The configurational entropy $S(x)$ was computed as the following:

$$S(x) = -k_B\left[\ln x + \frac{(1-x)\ln(1-x)}{x}\right]$$

where x stands for the Mg concentration defined simply as $x = \frac{n}{\#C\ atoms\ on\ graphene\ unit\ cell}$. All other contributions to the entropy are neglected, since the operating temperature is fixed to be at

room temperature. The free energy of the Mg cluster is then obtained using the following equation, with $\mu(Mg\ @\ C)$ fixed at x=8/50 concentration.

$$\Delta G(n) = E(n\ Mg\ on\ graphene) - E(graphene) - n \times \mu(Mg\ @\ C)$$

Surface energies (energies due to the dangling bonds on Mg atoms) are included in the energy terms obtained by *ab initio* computations and equilibrium crystal shapes are not considered for the small critical nucleus growth.

SAMPLE	MgH_2 (%)	Mg (%)
GO/Mg	96.0	4.0
rGO100/Mg	89.1	10.9
rGO200/Mg	84.6	15.4

Table S1. Quantitative analysis based on reference intensity ratio (RIR) method for a series of Mg composites after full absorption, showing partial absorption for the highly reduced GO/Mg due to coalesced and unencapsulated Mg particles.

SAMPLE	Mg Content (wt.%)
GO/Mg	92.3455
rGO100/Mg	89.1507
rGO200/Mg	91.5359

Table S2. The Mg content in the nanocomposites calculated by ICP-OES.

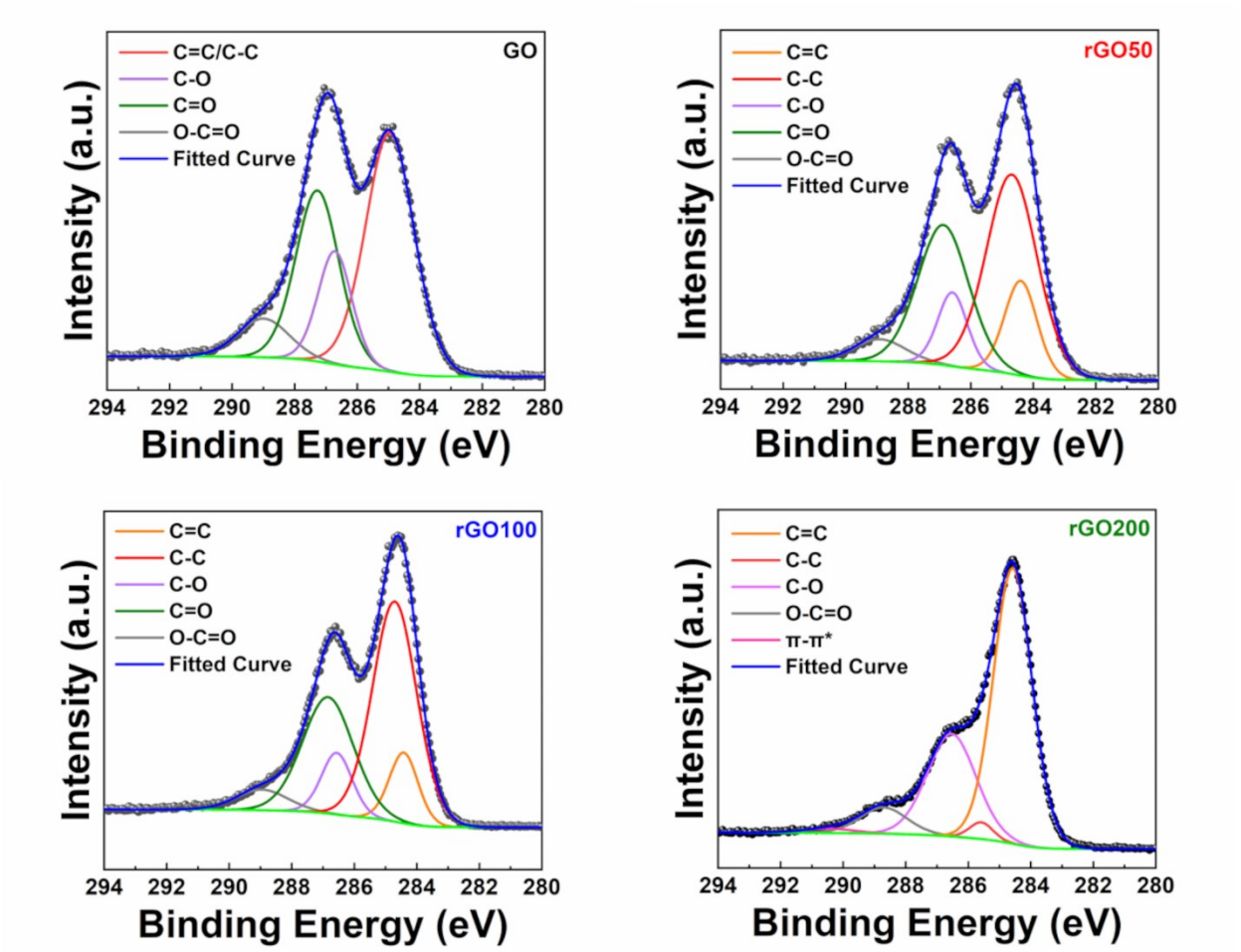

Figure S1. X-ray photoelectron spectra (C, 1s) of a series of reduced graphene oxides. The deconvolution shows the restoration of the graphitic structure as well as the diminution of oxygen-related peaks.

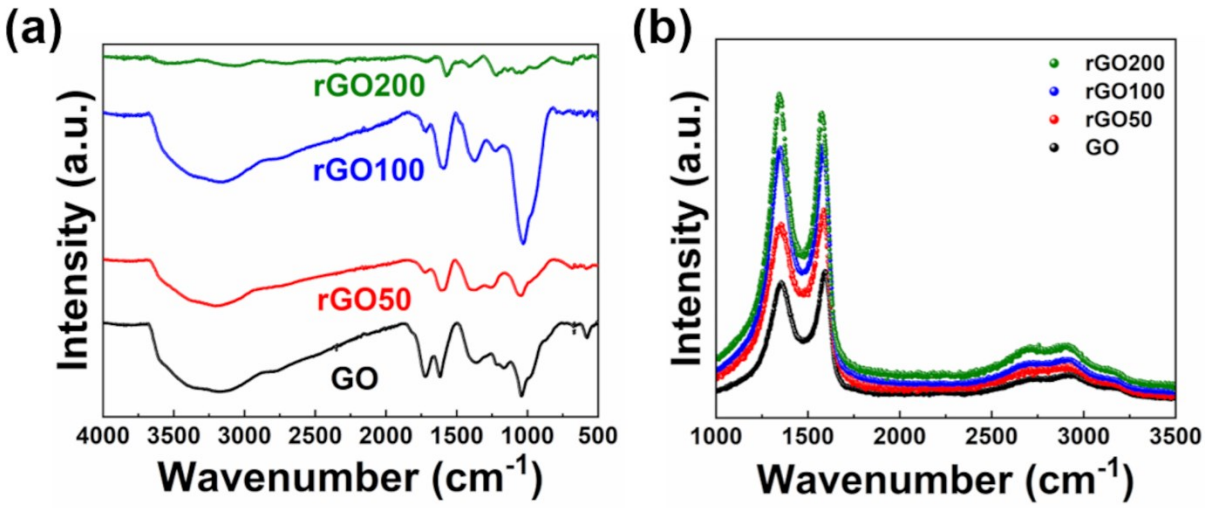

Figure S2. (a) FT-IR and (d) Raman spectra of GO and a series of rGOs. From FT-IR spectra, it is confirmed that the majority of oxygen-related peaks (O-H (~3200-3400 cm^{-1}), C=O (1725 cm^{-1}), C-OH (1380 cm^{-1}), C-O-C (1185 cm^{-1}), and C-O (1045 cm^{-1})) were diminished. The Raman spectroscopy shows an increased intensity ratio of D and G band peak, caused by decreased average domain size of sp^2 hybridized regions after chemical reduction.

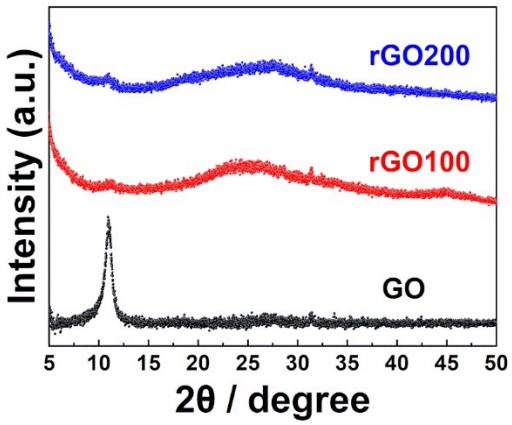

Figure S3. X-ray diffraction patterns of GO and rGOs, confirming the hierarchical reduction with interlayer distances.

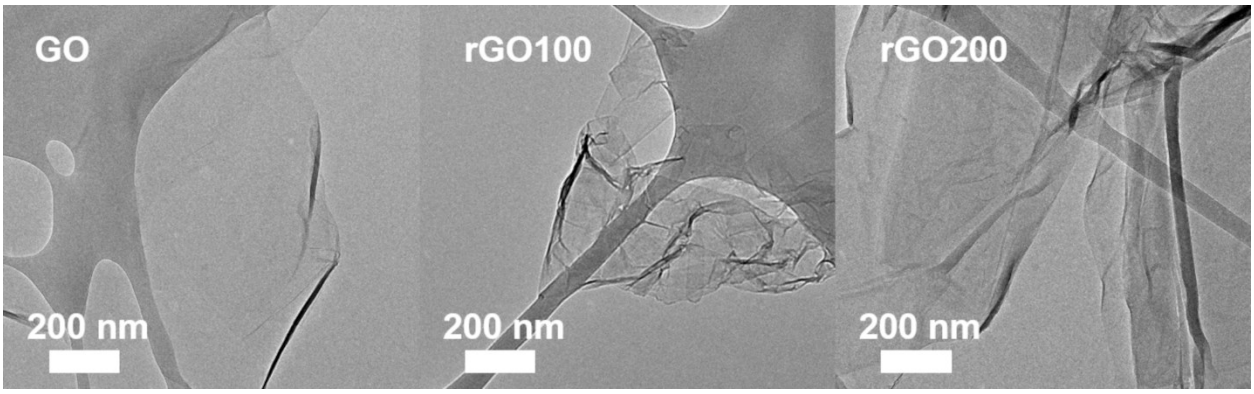

Figure S4. TEM images showing structural changes of GO sheets after the reduction process.

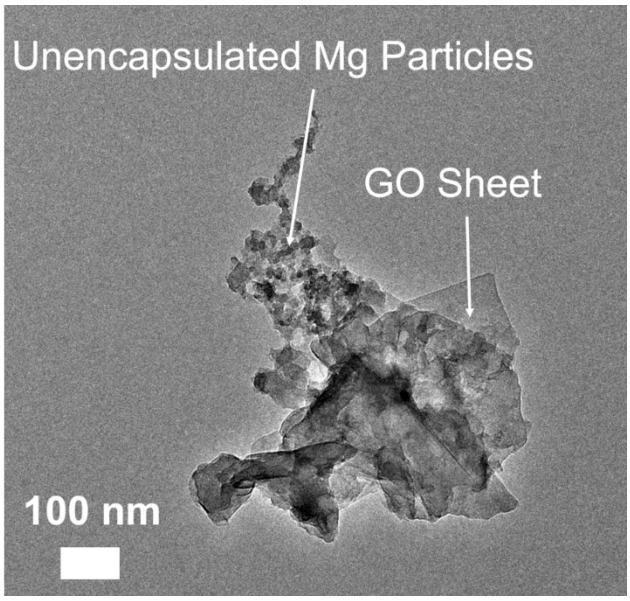

Figure S5. TEM image for rGO200/Mg showing unencapsulated Mg particles. The unencapsulated Mg particles are vulnerable to oxidation, leading to sluggish kinetics and decreased storage capacity.

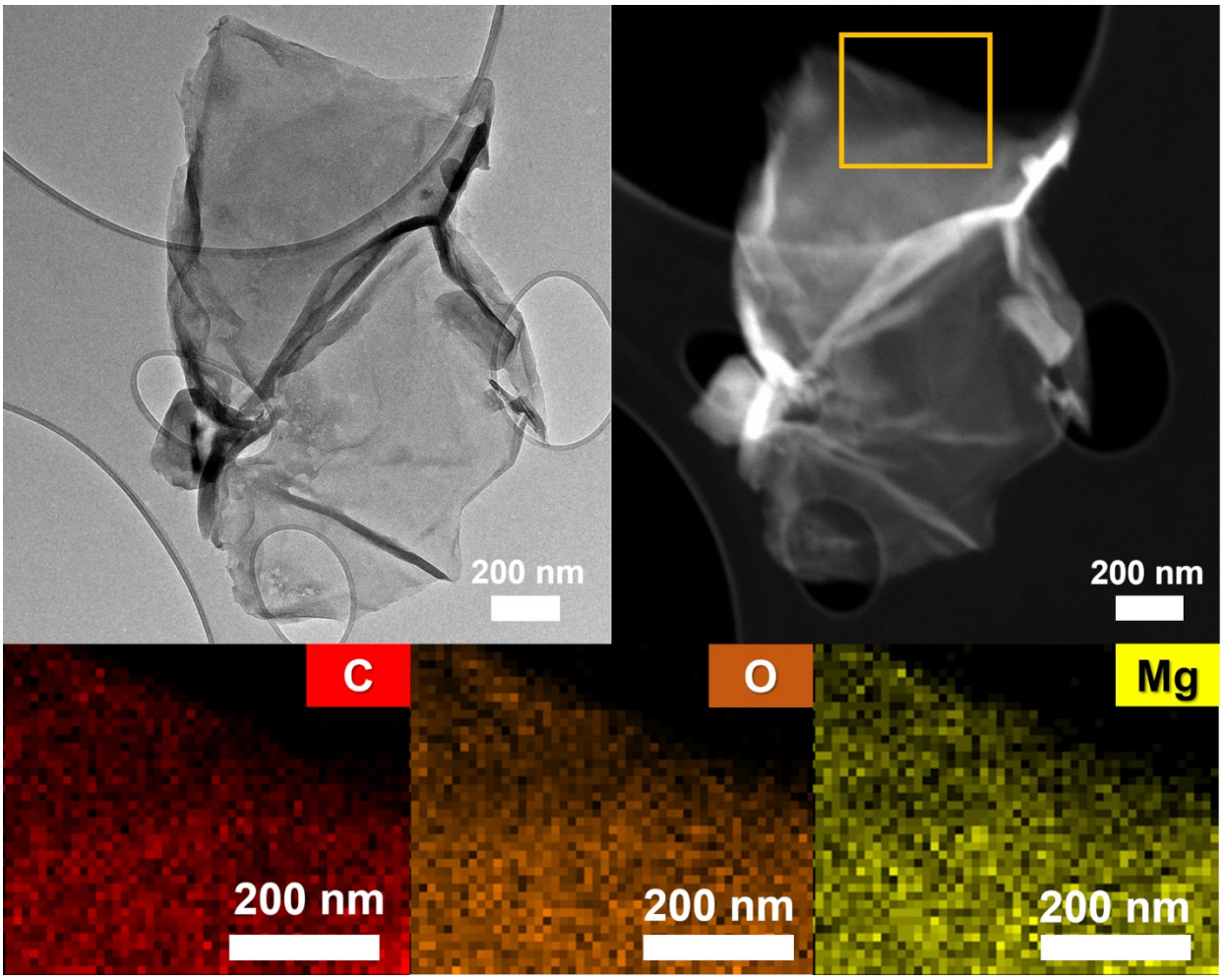

Figure S6. TEM EDS mapping for GO/Mg shows a homogeneous distribution of Mg nanocrystals over GO sheets. The coalesced Mg particles are hardly observed on the GO/Mg surface.

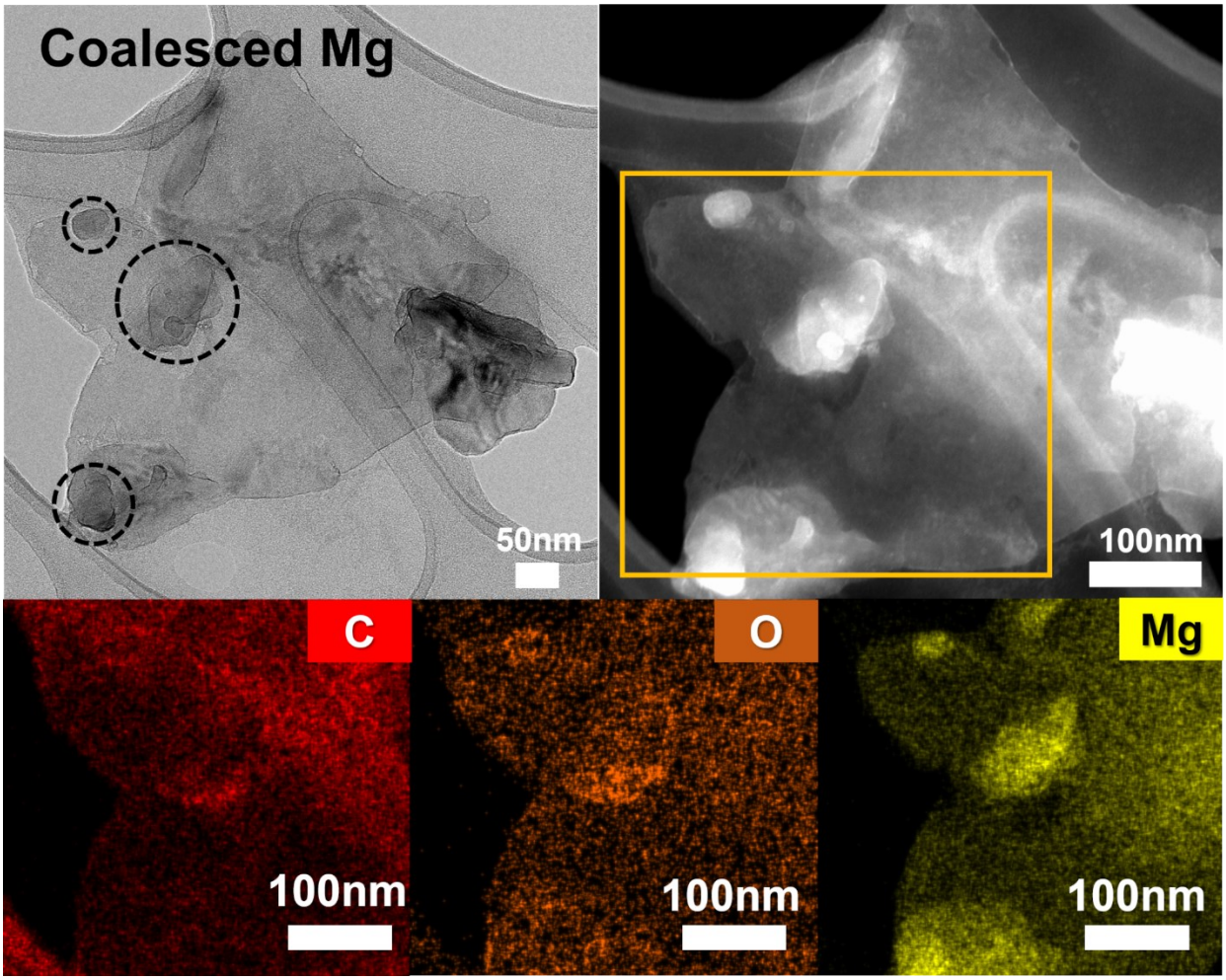

Figure S7. TEM EDS mapping for rGO100/Mg verifies formation of coalesced Mg particles (<100 nm) as well as Mg nanocrystals with 3-4 nm.

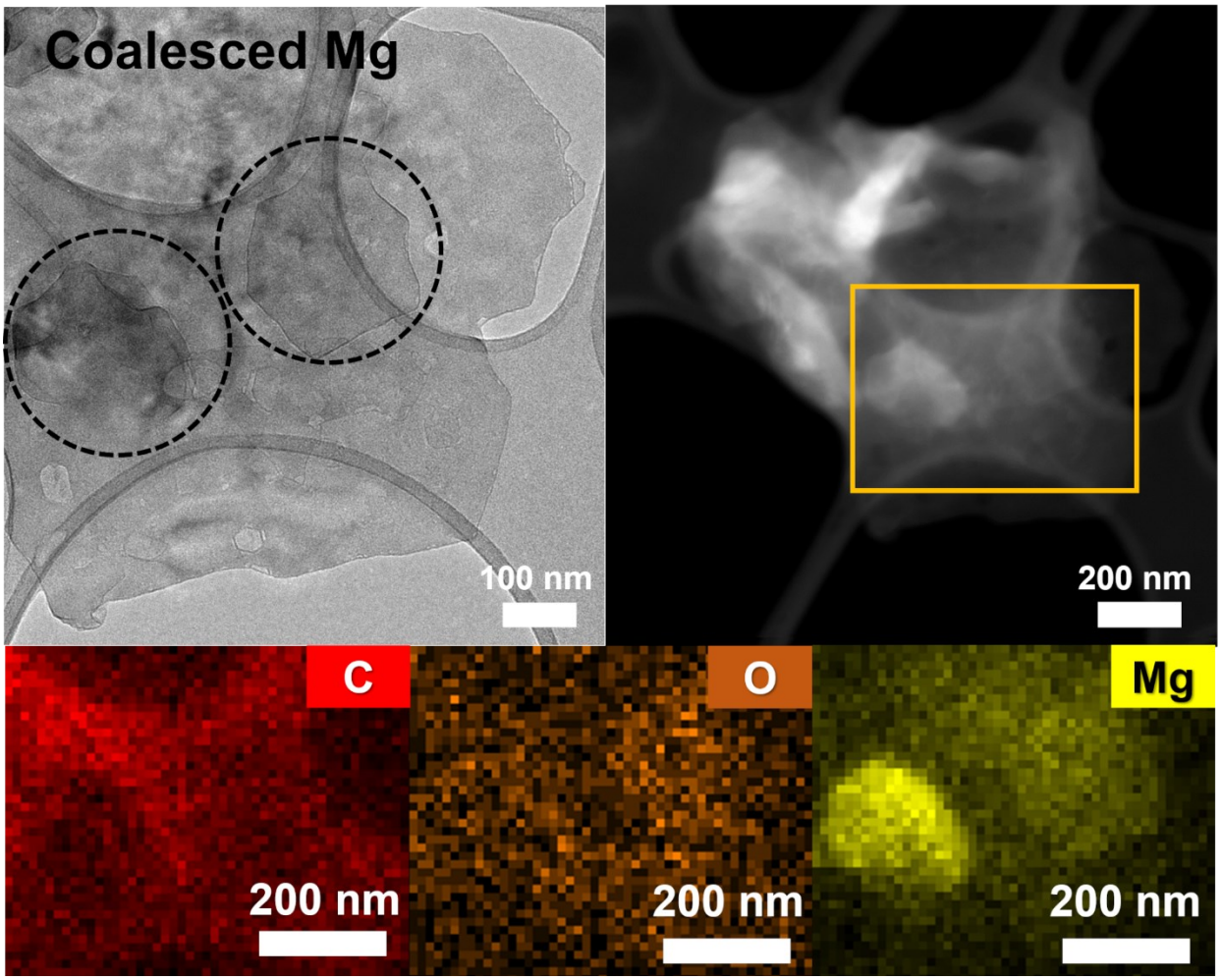

Figure S8. TEM EDS mapping for rGO200/Mg demonstrates the presence of relatively larger Mg particles (~200 nm) than rGO100/Mg.

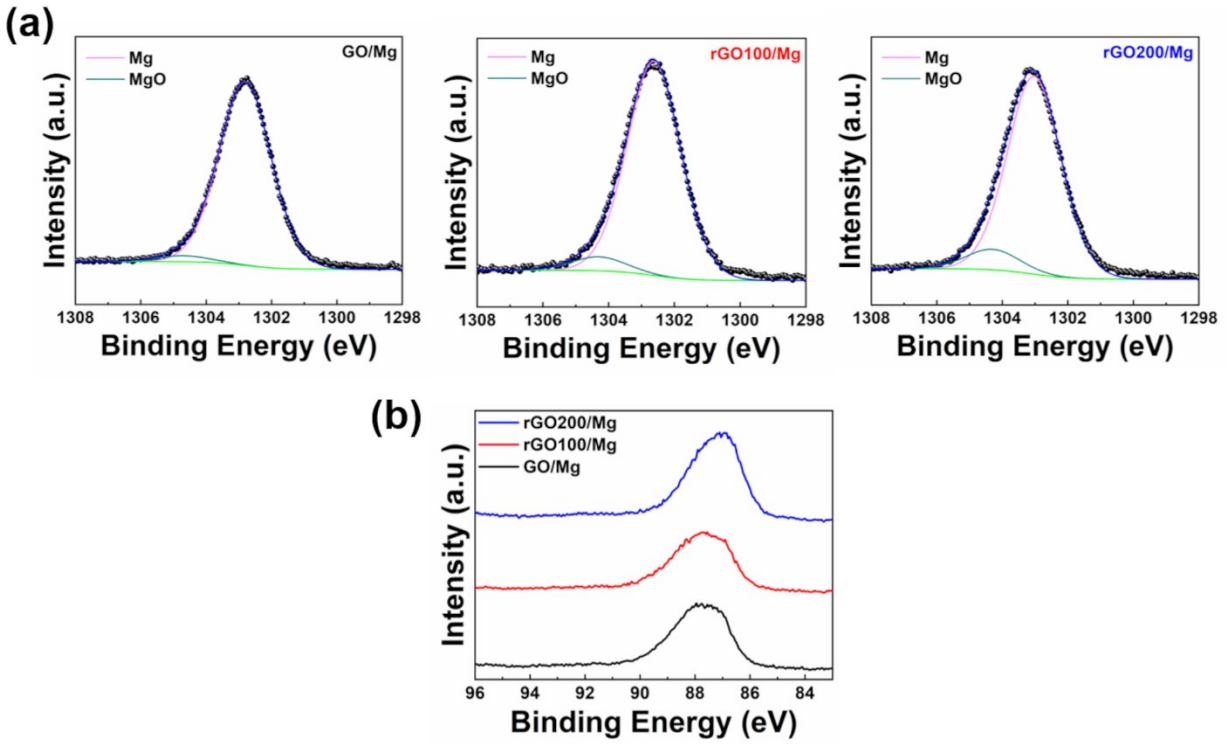

Figure S9. X-ray photoelectron spectra after synthesis: (a) Mg 1s (Mg at 1303 eV and MgO at 1304.5 eV), (b) Mg 2s (Mg at 88 eV, peak shift caused by the oxidation of the Mg particles). These Mg XPS spectrums suggest that more reduced GO/Mg composites have more coalesced Mg particles which are easily oxidized due to the absence of graphene layers.

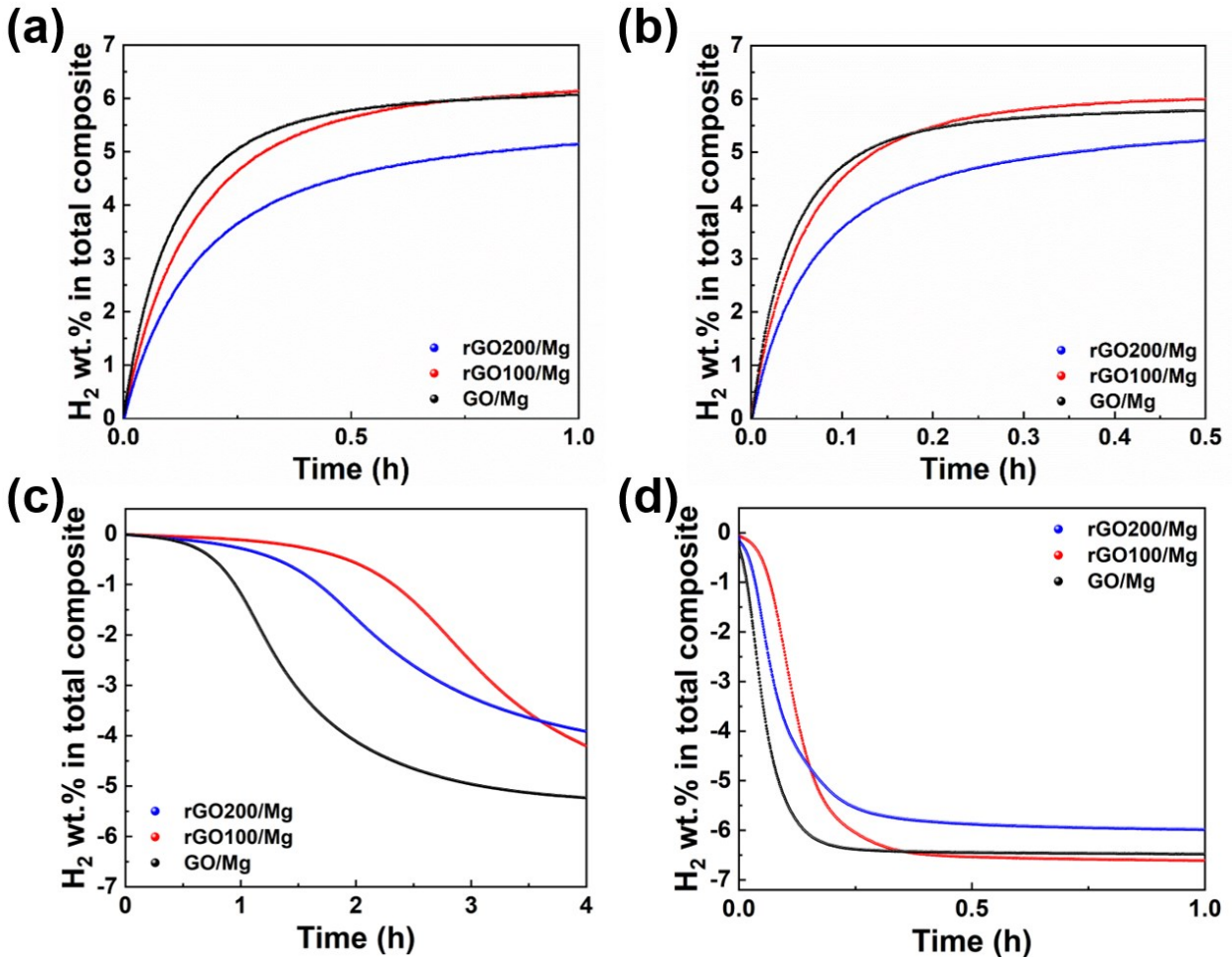

Figure S10. Hydrogen absorption at (a) 225℃ and (b) 250℃, and hydrogen desorption at (c) 275℃ and (d) 325℃, respectively.

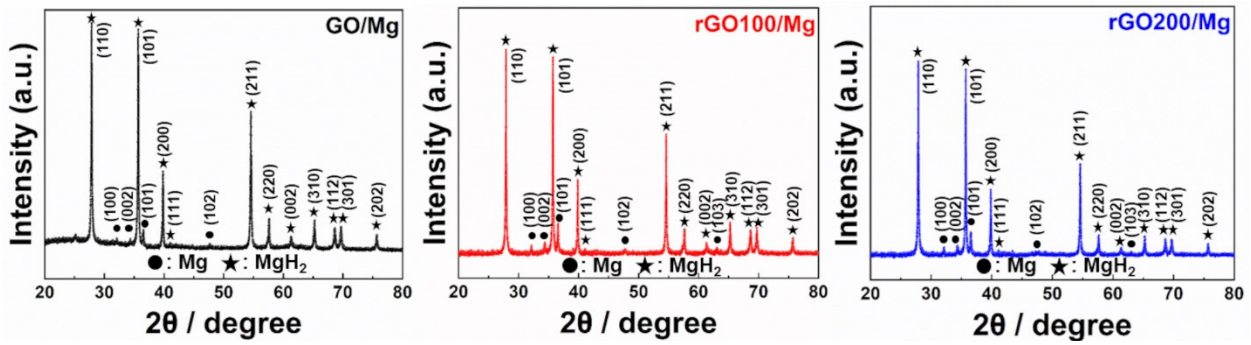

Figure S11. X-ray diffraction patterns of hydrogenated Mg composites, showing full absorption at 250 ℃, 15 bar.

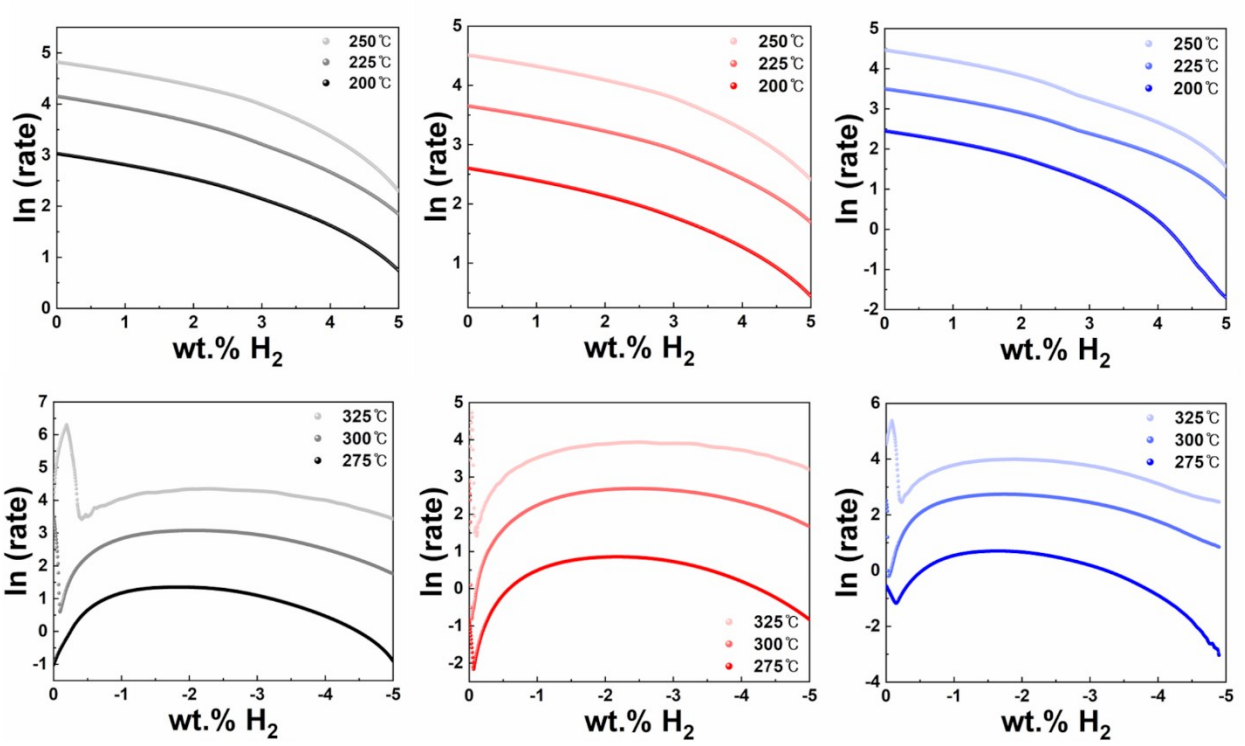

Figure S12. The change in the rate of absorption (top)/desorption (bottom) for (a) GO/Mg (black line), (b) rGO100/Mg (red line) and (c) rGO200/Mg (blue line), respectively.

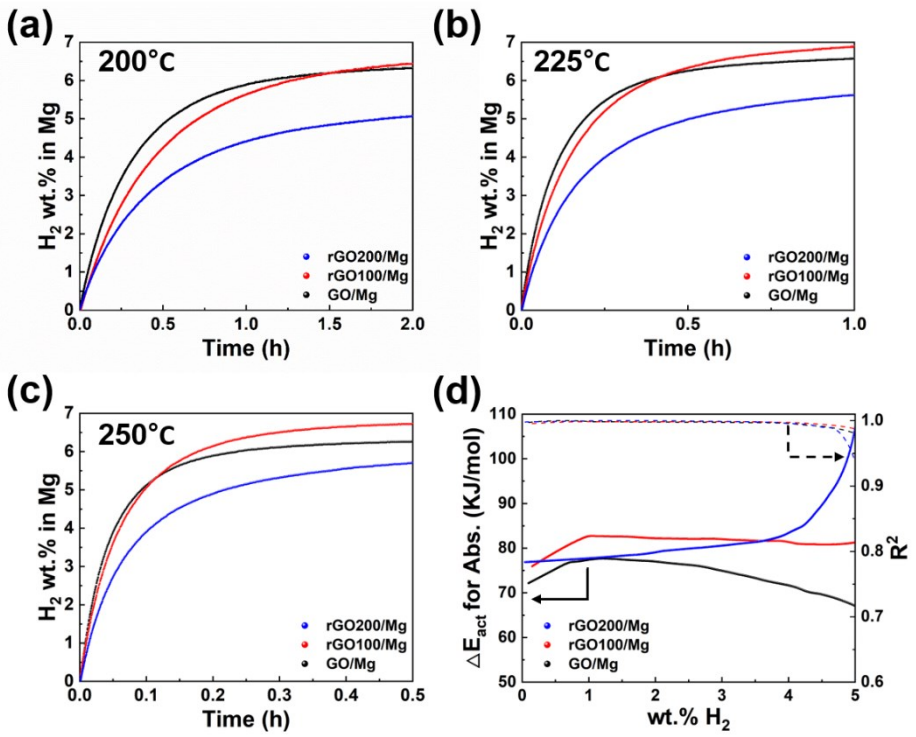

Figure S13. (a-c) Hydrogen absorption at 15 bar of H_2 at different temperatures (200, 225 and 250 °C, respectively); the capacity is calculated based on the Mg weight in the nanocomposites, (d) the change of activation energies and R^2 correlation values (dashed line) as a function of wt.% H_2 for absorption.

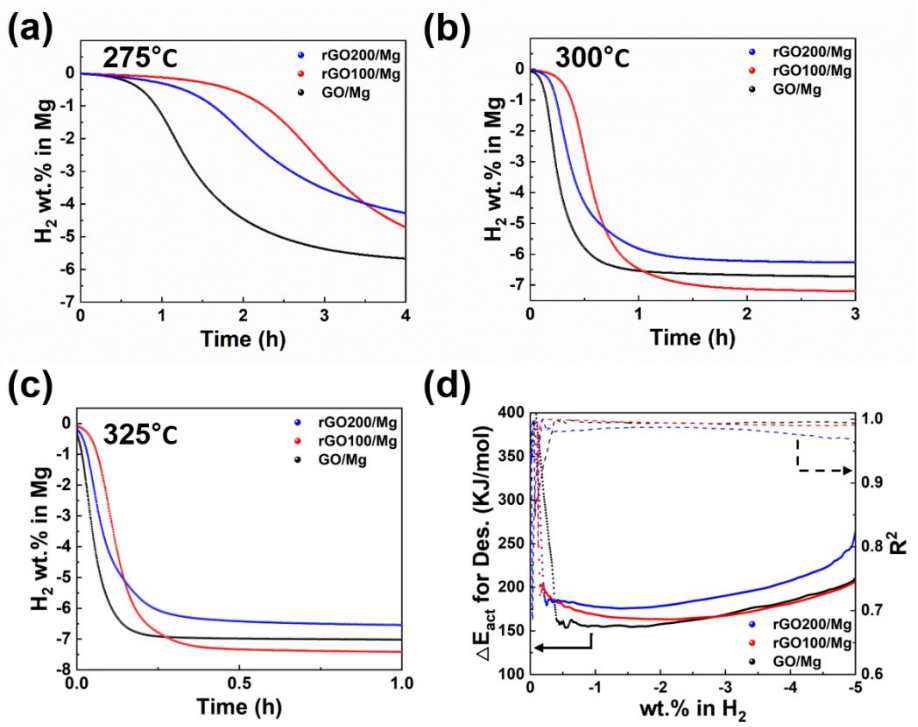

Figure S14. (a-c) Hydrogen desorption at 0 bar of H_2 at different temperatures (275, 300 and 325 °C, respectively); the capacity is calculated based on the Mg weight in the nanocomposites, (d) the change of activation energies and R^2 correlation values (dashed line) as a function of wt.% H_2 for desorption.

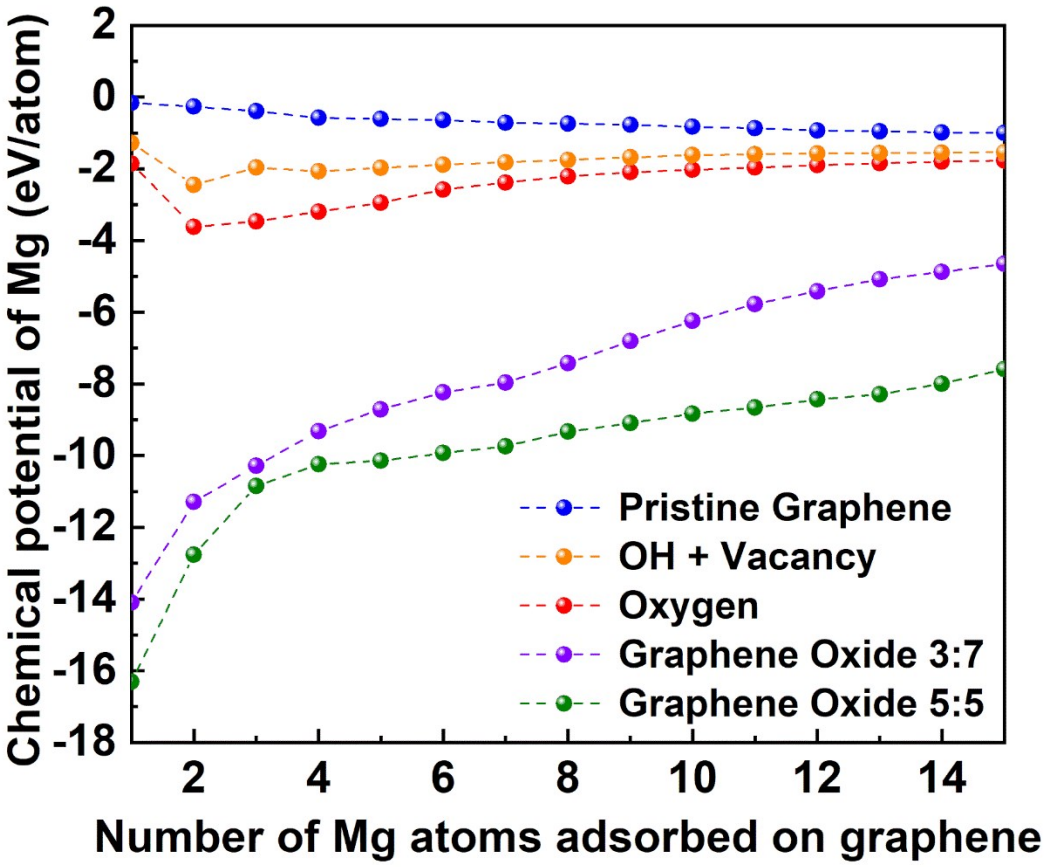

Figure S15. The chemical potential of adsorbed Mg on pristine, defected graphene and graphene oxides.

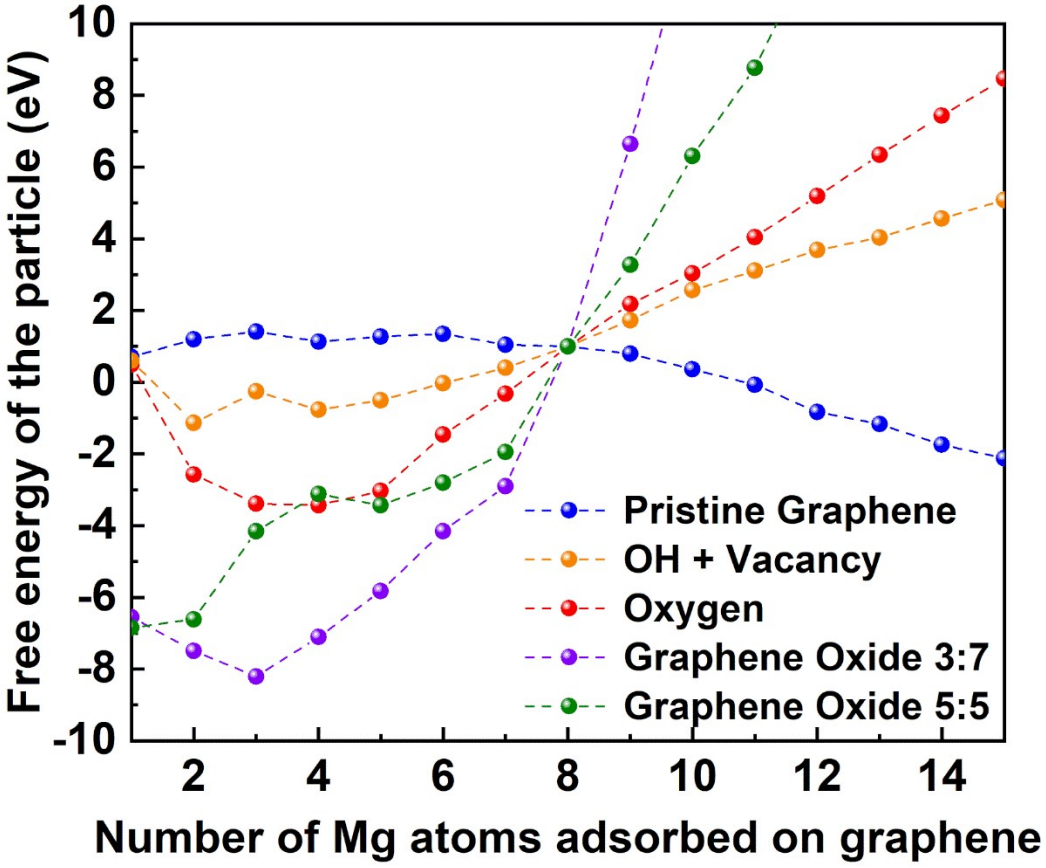

Figure S16. The free energy of the Mg cluster according to the number of Mg atoms adsorbed on graphene derivatives. The chemical potential of Mg is fixed to that at the Mg concentration of 8 Mg per 50 C at each graphene derivative.

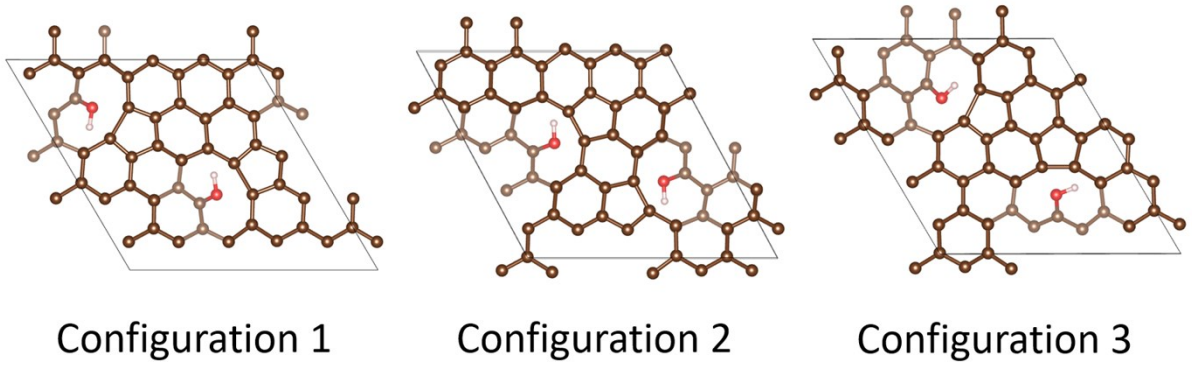

Figure S17. The initial hydroxide on C vacancy configurations at 2 defects per 50 carbon concentrations. Among the three, the second configuration exhibited the lowest energy and is thus selected for the subsequent Mg adsorptions.

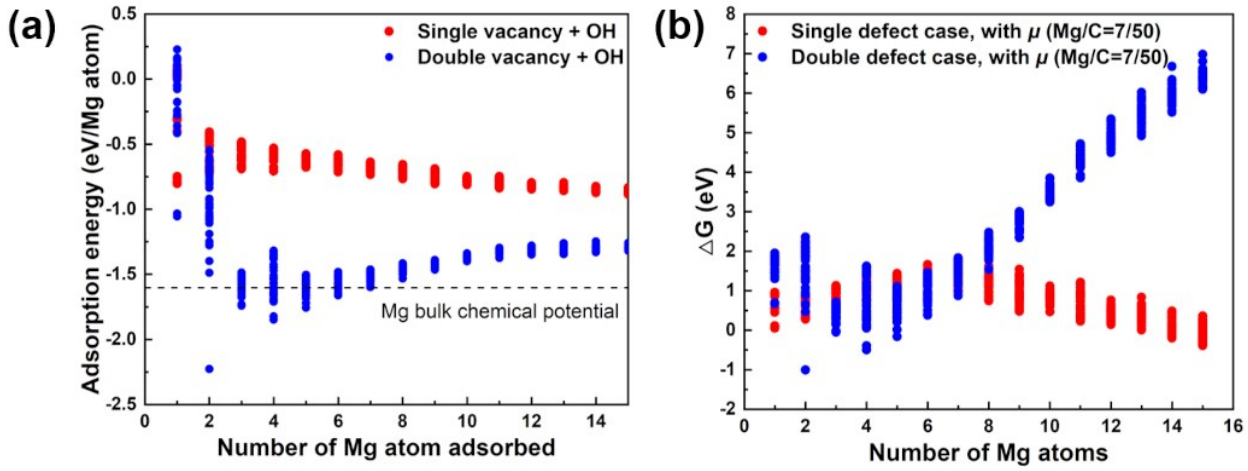

Figure S18. The configuration-dependent (a) Mg adsorption energy and (b) free energy of the Mg particle adsorbed on graphene derivatives.